# Efficient light harvesting in multiple-device stacked structure for polymer solar cells

Vishal Shrotriya, Elbert Hsing-En Wu, Gang Li, Yan Yao, and Yang Yang[a)]
*Department of Materials Science and Engineering, University of California Los Angeles, Los Angeles, California 90095*

We demonstrate a multiple-device stacked structure of polymer solar cells for efficient light harvesting. Two polymer photovoltaic cells are stacked together and connected in series or in parallel to achieve a tandem structure. In this two-cell structure, a multilayer semitransparent electrode, made of lithium fluoride (LiF)/aluminum (Al)/gold (Au), is used as the top contact in the bottom cell to efficiently transmit the unabsorbed photons to the upper cell. Maximum transparency of up to 80% is achieved for the semitransparent cathode. Upon stacking, the open-circuit voltage and the short-circuit current are almost doubled compared to a single cell. © *2006 American Institute of Physics.* [DOI: 10.1063/1.2172741]

Since the discovery of photoinduced charge transfer between organic donors and acceptors, great effort has been devoted to explore photovoltaic (PV) devices based on polymers.[1–8] To achieve high efficiency in these polymer PV devices, it is important that the solar radiation is absorbed efficiently in the active layer. To efficiently absorb the solar light, the thickness of the active layer has to be increased. However, the short charge carrier diffusion lengths (only a few nanometers) in these organic materials limit the thickness of the active layer.[9] As a result, only $\sim$30% of the total light is absorbed in the polymer layer[10] resulting in a lower than expected efficiency of the PV devices. Efficiency light harvesting has been demonstrated for organic solar cells utilizing tandem structure.[11,12] However for a polymer solar cell, achieving a tandem cell presents its own difficulties. Since the polymer film is solution processed, spincoating multiple layers in tandem can result in significant damage to the bottom layer from the solvent used for spincoating the subsequent layers. In this letter, we report on a multiple-device stacked structure, utilizing separate single PV cells with the help of a transparent electrode, in order to harvest an increased amount of photons which doubles the power conversion efficiency of these structures as compared to a single cell.

Several methods have been reported to obtain semitransparent cathodes for polymer light-emitting diodes (PLEDs), primarily focusing on two common techniques: Sputtering indium tin oxide (ITO) as the top cathode,[13,14] and using a multilayer stacked metal cathode.[15,16] Recently a semitransparent cathode was reported for PLEDs utilizing the multilayer stacked metal cathode.[17] In this work, we present a multilayer semitransparent cathode with optimized functionality in a multiple-device stacking structure. The two most important properties desired of a transparent cathode are transparency and efficient electron collection. LiF/metal and Ca/metal electrodes form efficient charge collection contact in polymer/methanofullerene solar cells.[18–20] We fabricated several types of semitransparent cathodes by using these materials, and the best cathode structure based on the optical and electrical properties is utilized in our multiple-device stacked structure. The most important properties for metal—that are taken into consideration while determining the cathode materials and structure in this study—are the skin depth, the electrical conductivity, and the wettability of the metal when thermally evaporated as a layer.

The polymer PV devices in this study consisted of a layer of polymer thin film sandwiched between the transparent anode ITO and a metal cathode. The active polymeric material is an admixture of poly(2-methoxy-5-(2′-ethyl-hexyloxy)-1,4-phenylene vinylene)] (MEH-PPV) and phenyl C61-butyric acid methylester (PCBM). The semitransparent and regular cathodes were obtained by thermally evaporating various metals, such as aluminum (Al), gold (Au), lithium fluoride (LiF), and calcium (Ca), under a vacuum of $10^{-6}$ Torr. The current-voltage (*I-V*) curves were obtained by a Keithley 2400 source-measure unit. The photocurrent was measured under illumination supplied by a ThermalOriel 150 W solar simulator (AM 1.5G). The thicknesses of the various films were measured using Dektak 3030 profilometer. All devices were tested in oxygen and moisture-free nitrogen ambient in the glove box.

In an Edisonian approach, several types of semitransparent cathodes were tried for their optical and electrical properties. The transmission spectra for these cathodes are shown in Fig. 1(a). The ultraviolet (UV)-visible absorption spectrum for the MEH-PPV/PCBM film is also shown in the figure for comparison. For measuring the transmission spectra for the cathode layer, 100% transmission baseline was collected for ITO/PEDOT:PSS/polymer layers. The different transparent cathodes that were tried include Ca(10 nm)/Al(10 nm), LiF(1 nm)/Al(10 nm), Ca(10 nm)/Au(12.5 nm), LiF(0.5 nm)/Au(12.5 nm), and LiF(1 nm)/Al(2.5 nm)/Au(12.5 nm). At the wavelength of 480 nm, which is the peak absorption wavelength of MEH-PPV as shown in the figure, the LiF/Al/Au cathode has maximum transmission (almost 75%). This cathode also has the highest overall transmission in the visible range (400–700 nm) with the maximum transmittance of up to 80% at 580 nm. Although the total thickness of the LiF/Al/Au cathode is more than the LiF/Au cathode (with an additional 2.5 nm Al layer in the former), the higher transparency is an interesting observation. This suggests that in-
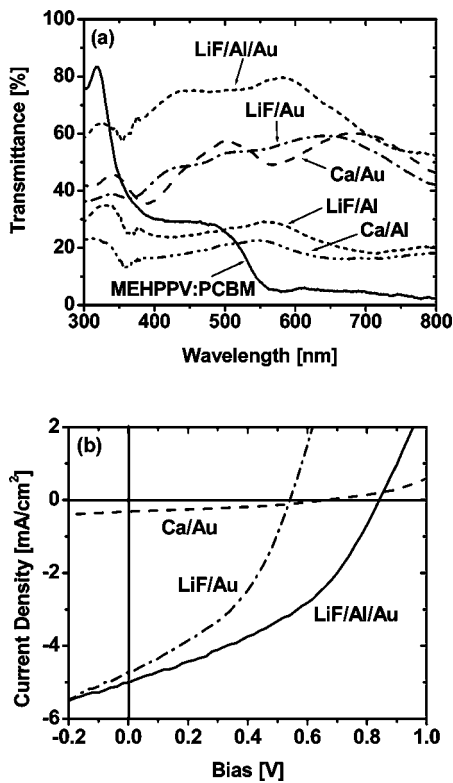
a)Electronic mail: yangy@ucla.edu

FIG. 1. (a) Transmittance spectra for different types of semitransparent cathodes: Ca(10 nm)/Al(10 nm), LiF(1 nm)/Al(10 nm), Ca(10 nm)/Au(12.5 nm), LiF(0.5 nm)/Au(12.5 nm), and LiF(1 nm)//Al(2.5 nm)/Au(12.5 nm). Also shown is the UV-visible absorption spectra for MEH-PPV:PCBM film for comparison. (b) *I-V* curves for polymer PV cells with three different types of semitransparent cathodes: Ca(10 nm)/Au(12.5 nm), LiF(0.5 nm)/Au(12.5 nm), and LiF(1 nm)/Al(2.5 nm)/Au(12.5 nm).
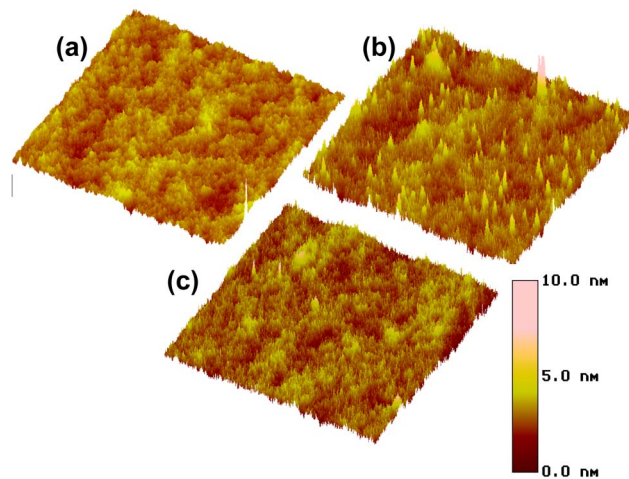


FIG. 2. AFM height images for (a) pristine polymer surface, (b) polymer surface covered with LiF (1 nm), and (c) polymer surface covered with LiF (1 nm) and Al (2.5 nm) layers. The images were obtained for a 5 $\mu$m $\times$ 5 $\mu$m surface area.

serting an extra metallic layer does not reduce the transparency of the cathode, but increases it instead. Not only is the transparency higher, but the performance of the device, as we will show from the *I-V* characteristics later, is much better for LiF/Al/Au. The higher transparency of LiF/Al/Au cathode is due to the role played by the Al layer in modifying the interface morphology between LiF and Au. We will come back to this discussion when we present the atomic force microscope (AFM)images later, but first we analyze the current density-voltage characteristics of devices using different semitransparent cathodes as shown in Fig. 1(b). Although the two LiF/Al and Ca/Al cathodes show much better electrical characteristics, they are excluded from the figure because of their poor transparency. The device with the LiF/Al/Au cathode showed the best performance in terms of short-circuit current ($I_{SC}$=5.0±0.1 mA/cm$^2$) and open-circuit voltage ($V_{OC}$=0.85 V), followed by the device with LiF/Au cathode ($I_{SC}$=4.7±0.2 mA/cm$^2$; $V_{OC}$=0.55 V), and finally the Ca/Au cathode ($I_{SC}$=0.3±0.05 mA/cm$^2$; $V_{OC}$=0.64 V). LiF lowers the work function of the Al due to the strong dipole moment of LiF (Ref. 21) and, as a result, the open-circuit voltage for the device with a LiF/Al/Au cathode is 0.8 V, compared to only 0.6 V for the LiF/Au cathode.

To understand the reason for higher transparency of the optimized cathode, we obtained AFM height images of the active layer after successive evaporation of LiF and Al layers. The AFM images are presented in Fig. 2. The pristine polymer surface is very smooth with a root-mean-square (rms) roughness ($\sigma_{rms}$) of 0.46 nm [Fig. 2(a)]. When a very

thin interfacial layer of LiF (thickness $\sim$ 1 nm) is evaporated on top of the polymer layer, it cannot cover the entire polymer surface to form a contiguous film. Instead, it forms segregated islands, as seen in Fig. 2(b), thereby increasing the active layer surface roughness ($\sigma_{rms}$=0.79 nm). However, depositing an additional 2.5 nm Al layer makes the surface smoother compared to when only LiF is present, and the rms roughness reduces to 0.55 nm which is comparable to the roughness of the pristine polymer layer. One of the important factors that govern the optical transparency is the wettability of the metal film onto the surface underneath. In this case, the Au film evaporated on top of LiF/Al will have much better wettability and will form a continuous film free of voids. When Au is evaporated directly on top of LiF (without the Al layer) the film thus formed will be rough will many voids. These voids act as scattering sites for the light waves, therefore reducing the transparency of the film. The LiF/Al/Au film will therefore have a better optical transparency than the LiF/Au film. Another factor that determines the optical transparency of a film is the skin depth, $\delta$. Au has a $\delta$ of 20 nm compared to only 6 nm for Al.[22] Therefore, for the same thickness of the film, Au will be more transparent. In the LiF/Al/Au cathode, the thickness of the Al layer is only 2.5 nm. Also, a thin Al layer will probably get oxidized readily to form aluminum oxide, which is transparent. All three factors discussed above will result in higher transparency for a LiF/Al/Au cathode, which is selected as the top cathode in our multiple-device stacking structure.

After the semitransparent cathode has been obtained, two separate PV devices can be stacked together to form a multiple-device stacking structure. The devices are stacked on top of each other and can be connected in series or in parallel to enhance the voltage or current output, respectively. Both devices are illuminated together using a single source with an intensity of 100 mW/cm$^2$ under AM 1.5G conditions. The light from the source is absorbed partially by the first PV device (PV1), and the unabsorbed photons are transmitted through the semitransparent cathode (LiF/Al/Au) to the second device (PV2) where they are absorbed by the second active layer. Both active layers consisted of MEH-PPV/PCBM with the layer thickness of $\sim$70 nm. *I-V* curves were measured for the stacked devices
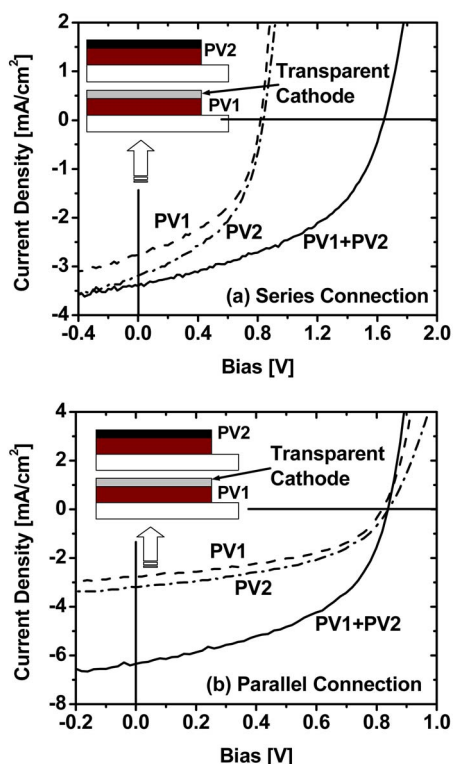
FIG. 3. *I-V* curves for the multiple-device stacked structures where the two cells were connected in (a) series and (b) parallel. Also shown are the *I-V* curves measured for individual cells PV1 and PV2. The stacking sequence for the devices PV1 and PV2 are shown in the inset of both figures.

connected in series and in parallel, and the typical results are shown in Figs. 3(a) and 3(b), respectively. First, the *I-V* curves were measured for devices PV1 and PV2 separately. The short-circuit current density ($J_{SC}$), the open circuit voltage ($V_{OC}$), and the fill factor (FF) are 2.6 mA/cm$^2$, 0.86 V, and 0.45 for PV1, and 3.2 mA/cm$^2$, 0.86 V, and 0.45 for PV2. The variation in $I_{SC}$ was ±0.15 mA/cm$^2$ for PV1 and ±0.10 mA/cm$^2$ for PV2. No significant variation in FF was observed for the two types of devices. For PV1, the variation in $V_{OC}$ was ±0.02 V; and for PV2, no significant variation in $V_{OC}$ was observed. The *I-V* curve for PV2 was measured with device PV1 kept in front and allowing the light to pass thorough it before reaching PV2, so as to make a fair comparison when the stacked devices were measured. After stacking devices PV1 and PV2 and connecting them in series, the device operating parameters for the stacked structure are $I_{SC}$=3.4 mA/cm$^2$, $V_{OC}$=1.64 V, and FF=0.45. Therefore, the $V_{OC}$ for the stacked structure doubled, whereas the $I_{SC}$ and FF remained more or less unchanged. Based on several devices that were measured, the variation in $I_{SC}$ was ±0.20 mA/cm$^2$; in $V_{OC}$, was ±0.02 V. For the stacked structure with parallel connection, the parameters were $I_{SC}$ =6.3 mA/cm$^2$, $V_{OC}$=0.84 V, and FF=0.45 with a variation of ±0.1 mA/cm$^2$ in $I_{SC}$ and ±0.02 V in $V_{OC}$. In this case, the value of $I_{SC}$ doubled, whereas $V_{OC}$ and FF remained unchanged compared to PV1 and PV2. As a result of stacking, the power conversion efficiency for the stacked structures were 2.4±0.2% (in series) and 2.5±0.1% (in parallel) compared to ∼1.1% and ∼1.3% for PV1 and PV2, respectively.

Thus, the efficiency can be more than doubled when individual PV cells can be stacked together. In this work, we used the same active layer for both PV1 and PV2 in order to efficiently absorb the photons that remain unabsorbed from the first active layer. However, this technique can be extended to use materials with different peak absorption wavelengths in order to increase the total absorption range of the stacked device structure and cover a larger part of the solar spectrum.

In conclusion, we have demonstrated a multiple-device stacked structure for efficient light harvesting in polymer solar cells. Two polymer PV cells, one of them capped with a semitransparent cathode, are stacked to form a tandem structure. The $I_{SC}$ and $V_{OC}$ can be doubled compared to a single cell when the cells are stacked together and connected in parallel or in series, respectively. This multiple-device stacked structure overcomes the limitations of using a tandem cell for solution processable polymer solar cells. The highest power conversion efficiency of up to 2.6% was achieved for the multiple-device stacked structure.

[1] C. J. Brabec, N. S. Sariciftci, and J. C. Hummelen, Adv. Funct. Mater. **11**, 15 (2001).

[2] K. M. Coakley and M. D. McGehee, Chem. Mater. **16**, 4533 (2004).

[3] C. J. Brabec, Sol. Energy Mater. Sol. Cells **83**, 273 (2004).

[4] S. E. Shaheen, C. J. Brabec, N. S. Sariciftci, F. Padinger, T. Fromherz, and J. C. Hummelen, Appl. Phys. Lett. **78**, 841 (2001).

[5] F. Padinger, R. S. Rittberger, and N. S. Sariciftci, Adv. Funct. Mater. **13**, 85 (2003).

[6] C. Walduf, P. Schilinsky, J. Hauch, and C. J. Brabec, Thin Solid Films **451**, 503 (2004).

[7] G. Li, V. Shrotriya, J. Huang, Y. Yao, T. Moriarty, K. Emery, and Y. Yang, Nat. Mater. **4**, 864 (2005).

[8] M. L. Ma, C. Y. Yang, X. Gong, K. Lee, and A. J. Heeger, Adv. Funct. Mater. **15**, 1617 (2005).

[9] P. Peumans and S. R. Forrest, Appl. Phys. Lett. **79**, 126 (2001).

[10] Calculated from Beer's law: $A=\log_{10}(1/T)$, where $A$ is the absorbance and $T$ is the transmittance. Absorbance was calculated for MEH-PPV:PCBM films from UV-visible absorption spectra shown in Fig. 1(a).

[11] M. Hiramoto, M. Suezaki, and M. Yokoyama, Chem. Lett. **1990**, 327 (1990).

[12] A. Yakimov and S. R. Forrest, Appl. Phys. Lett. **80**, 1667 (2002).

[13] L. S. Hung and C. W. Tang, Appl. Phys. Lett. **74**, 3209 (1999).

[14] G. Pathasarathy, P. E. Burrows, V. Khalfin, V. G. Kozolov, and S. R. Forrest, Appl. Phys. Lett. **72**, 2138 (1998).

[15] L. S. Hung, C. W. Tang, M. G. Mason, P. Raychaudhuri, and J. Madathil, Appl. Phys. Lett. **78**, 544 (2001).

[16] R. B. Pode, C. J. Lee, D. G. Moon, and J. I. Han, Appl. Phys. Lett. **84**, 4614 (2004).

[17] E. H.-E. Wu, S. H. Li, C.-W. Chen, G. Li, Z. Xu, and Yang Yang, IEEE/OSA J. Display Technology **1**, 105 (2005).

[18] C. J. Brabec, S. E. Shaheen, C. Winder, and N. S. Sariciftci, Appl. Phys. Lett. **80**, 1288 (2002).

[19] F.-C. Chen, Q. Xu, and Y. Yang, Appl. Phys. Lett. **84**, 3181 (2004).

[20] G. Li, V. Shrotriya, Y. Yao, and Y. Yang, J. Appl. Phys. **98**, 043704 (2005).

[21] W. J. H. van Gennip, J. K. J. van Duren, P. C. Thüne, R. A. J. Janssen, and J. W. Niemantsverdriet, J. Chem. Phys. **117**, 5031 (2002).

[22] R. A. Chipman, *Theory and Problems of Transmission Lines*, Schaum's Outline Series (McGraw–Hill, New York, 1968).